

## A Comparison of Fiducial Shapes for Machine Vision Registration

Lawrence O'Gorman

Alfred M. Bruckstein

Chinmoy B. Bose

Israel Amir

AT&T Bell Laboratories  
Murray Hill, New Jersey 07974

### ABSTRACT

One way to perform registration and alignment for machine assembly is with respect to precisely located landmarks, called fiducials, that are located by machine vision means. For applications such as electronics assembly, where densities are high and tolerances must be low, the precision by which the fiducials are located affects everything aligned relative to them. Because of spatial sampling effects, differently shaped fiducials can be measured with different levels of precision. In past work we have determined and compared the minimax precision error for simple geometric shapes, and extended the results to propose a concentric pattern as having desirable qualities of high location precision and rotational invariance. We reiterate this work, and extend it to examine the performance of the concentric fiducial, as a function of diameter, number of rings, noise, and ring spacing.

### 1. Introduction

Electronics assembly, robotics manipulation, and many other manufacturing applications, require precise registration to assure proper positioning and alignment. One way to perform registration is to position everything with respect to one or more landmarks, called *fiducial marks*, or simply *fiducials*. For the electronics application, fiducials are positioned in precise and known locations relative to circuit traces. Then registration is performed relative only to the fiducials, independent of any imprecision of absolute positioning on the machine. In this paper, we reiterate past work [1], on determining the minimax precision of simple geometrically shaped fiducials, and extend our examination of a concentric pattern, which was proposed in [2] as having desirable fiducial characteristics.

In this paper, location is measured by the centroid calculation. Because this measurement is performed on spatially sampled data, there may be a difference between the true (unsampled) centroid location and that measured from the pixels. The Euclidean distance, measured in units of pixels, between the true and measured centroid of a fiducial is called the precision error. There are other methods for determining location, which are reviewed in reference [2], but the centroid calculation has an advantage that it is simple and fast. Besides work on registration, there is also a body of work in the area of subpixel precision that is applicable to this paper. Many of these papers have also been referenced in [2] but for completeness we mention reference [3] on imprecision regions (called "locales") due to spatial sampling, references [4-5] on digital disks and rings, and a more recent paper [6], dealing with the effects of noise on locale shape and size.

### 2. Shape and Size of Simple Geometric Fiducials

In an earlier work [1] the subpixel registration precision of simple geometrically shaped fiducials was studied. Using analysis and experiment, the maximum error in the centroid due to spatial sampling was examined for different shapes and parameters. For completeness, we summarize this work here.

For purposes of analysis and experiment, the image is assumed to be binary. The binary images are created by assigning a 1 to a pixel  $p(x,y)$  if its center is found to be within

the analog fiducial region, and 0 otherwise. For determination of the effects of sampling, the center of the concentric fiducial was shifted uniformly within (0,0) to (0.5,0.5) at increments of 0.01 pixels in  $x$  and  $y$ . The maximum of the errors for all ( $50 \times 50 = 2500$ ) shifts within this region is found and recorded. To test the effects of size, a dimension of the fiducial is incremented in 0.25 pixel steps over a range of 2 to 22 pixels, and the change of error is examined.

Results in Figure 1 show the precision error plotted against the size (sidelength for square, vertical diagonal for diamond with other diagonal fixed, and diameter for circle). It can be seen here, and is explained in more detail in references [1-2], that, while the precision error for the square is at best, 0.25 pixels, both the diamond and circle have errors that decrease with larger size. While none of the plots decrease monotonically, that of the diamond has very large deviations from minimum whereas the circle has smaller local maxima. This non-monotonicity in the decrease of the error curve is due to the spatial sampling effects between the Cartesian grid and the continuous shape. For the diamond shape, rotation of a fixed-size shape produces similar effects. In the following sections, we choose to develop and expand upon use of the circular shape as a fiducial because of its relatively small and low-deviation error as shown in Figure 1, and because its shape is rotationally invariant.

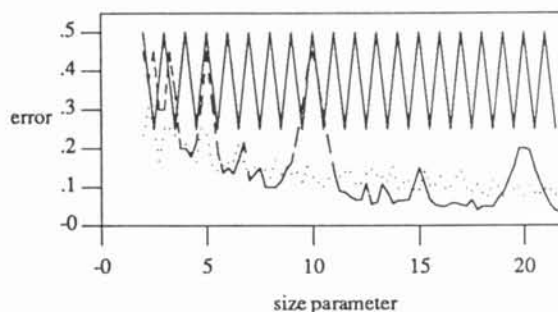


Figure 1. Maximum sampling error for the centroids of the square (solid line), diamond shape (dashed), and circular disk (dotted), over different lengths of sidelength, vertical diagonal, and diameter, respectively.

### 3. Centroid Calculations and the Concentric Fiducial

In this section, we review the development from circular to concentric fiducial. This development is made by modifying the centroid calculation method. The most straightforward method of centroid determination is just to find the average of the 1-pixel locations,  $(M_x, M_y)$ :

$$M_x = \frac{1}{A} \sum_y \sum_x x \cdot p(x,y), \quad M_y = \frac{1}{A} \sum_y \sum_x y \cdot p(x,y). \quad (1)$$

$$\text{where } A = \sum_y \sum_x p(x,y). \quad p(x,y) = \{0,1\}.$$

Knowledge of the fiducial size and shape can be exploited to improve the measure. Consider that it is not necessary to sum all the pixels within the fiducial; instead, with knowledge that the disk is filled (completely 1-valued), the edges can be found, and the same centroid calculated just from these edge locations. For the edges of  $x$ -runs starting at  $x_c(y)$  and ending at  $x_f(y)$  for rows of  $y$ , the centroid and area can be calculated:

Address correspondence to the first author at AT&T Bell Laboratories, Rm. 3D-455, Murray Hill, NJ, 07974. A.M. Bruckstein is visiting from the Technion, IIT, Israel.

$$M_x = \frac{1}{A} \sum_y \sum_{x=x_o(y)}^{x_f(y)} x \cdot p(x,y)$$

$$= \frac{1}{2A} \sum_y \left[ x_f^2(y) + x_f(y) - x_o^2(y) + x_o(y) \right] \quad (2)$$

$$A = \sum_y \left[ x_f(y) - x_o(y) + 1 \right]$$

When the centroid is determined from equation (2), the inside pixels are not used. Therefore, we can change the values within the disk edges without affecting this centroid calculation. We take advantage of this to change the inside pixels in such a way as to improve the estimate of the centroid. It was shown in reference [2] that the variance of the centroid calculated over greater than one disk is smaller than that on a single disk (where the maximum diameters are the same). Adopting the philosophy that "the more fiducials, the better", we insert into the original disk, more disks, all concentric, of a sequence of uniformly increasing radii from the inner to outer disks, and of alternating 1,0 values, as in Figure 2. We determine the centroid of each disk, treating them as filled either with 1 or 0 values. Then the weighted average of these  $r$  centroids is found, and said to be the centroid of the concentric fiducial. From reference [7], where the variance is shown to decrease linearly with increasing disk diameter, we choose to weight the moments of each disk proportionally to their respective diameters,  $d(i)$ . Therefore, we define the centroid for the combination of disks in the concentric pattern as,

$$M_x = \frac{1}{\sum_i d(i)} \sum_i d(i) M_x(i) \quad i = 1, 2, \dots, r \quad (3)$$

where  $M_x(i)$  is calculated as for  $M_x$  in equation (2).

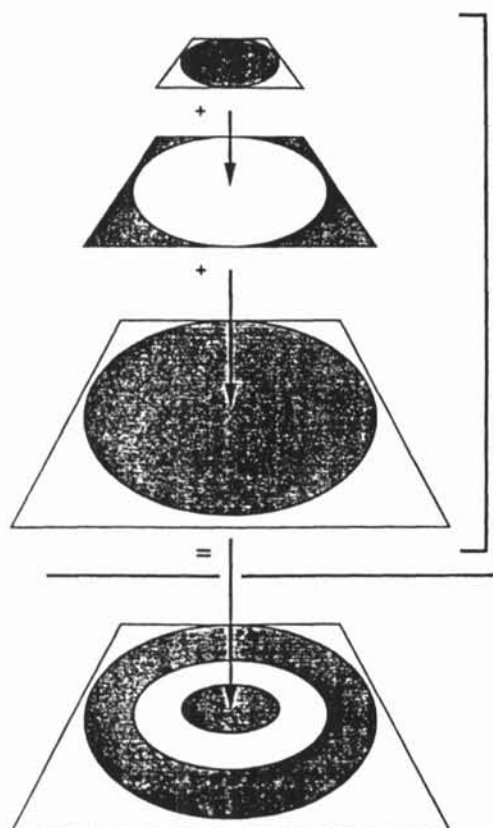


Figure 2. A fiducial with three rings can be thought of as the concentric superposition of all the disks. The area of the fiducial is that of the largest disk, but the effective area is the sum of individual disks.

The advantage of this concentric configuration is that more fiducials have been added but *all additional disks are contained in the area of the original disk*. When each ring of the concentric fiducial is considered as a filled disk, we refer to the total area of these disks as their *effective area*,  $A_E$ . The effective area for  $r$  disks is,

$$A_E = \sum_{i=1}^r A(i) = \sum_{i=1}^r \sum_y \left[ x_f(y) - x_o(y) + 1 \right]_i \quad (4)$$

For a fixed diameter,  $d$ , the increase in effective area with the number of rings results in a decrease of effective variance. We show this below. For a concentric fiducial of  $r$  independent disks, the effective variance is,

$$\sigma_E^2 = \sum_i \left[ \frac{d(i)}{\sum_i d(i)} \right]^2 \sigma_i^2 \quad (5)$$

where  $\sigma_i$  is the variance of each disk. It is shown by Monte Carlo simulation in [7] that the variance of the centroid estimate for a single disk is  $\sigma_i^2 = k / d_i$ , where  $k$  is a constant. For the outer ring whose diameter is  $d$ , the variance is  $\sigma^2 = kd$ . Therefore expressing the variance for each ring with respect to that for the outer,

$$\sigma_i^2 = \frac{d}{d_i} \sigma^2 \quad i = 0, \dots, r-1 \quad (6)$$

Substituting this in equation (5),

$$\sigma_E^2 = \frac{\sigma^2 d}{\sum_i d(i)} \quad (7)$$

Substituting for  $d_i = (2i-1)d / (2r-1)$ , and simplifying, then

$$\sigma_E^2 = \frac{2r-1}{r^2} \sigma^2 \quad (8)$$

The effective variance, normalized by the variance for the outer disk, is plotted in Figure 3. It can be seen that the effective variance is always less than or equal to  $\sigma^2$ , and that it decreases for larger  $r$  with the inverse relationship approximately  $2/r$ .

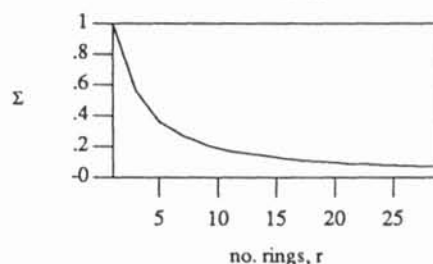


Figure 3. The plot shows that the variance decreases with the number of rings, where the normalized variance is  $\Sigma = \sigma_E^2 / \sigma^2$ .

#### 4. Concentric Ring Diameters

In Section 3, the assumption was that the rings were spaced uniformly apart. In this section, we examine whether the relative spacing between rings has an effect upon the error in the centroid measurement. We extend results of the one-dimensional case examined elsewhere (in a currently unpublished paper) to this two-dimensional application, and test the different ring spacings in the next section.

If a one-dimensional cross-section is taken from the center of a concentric fiducial, this yields a sequence of runs of 1s and 0s for each ring. Consider first a continuous function,  $f(x)$ ,  $x \in R$ , having a sequence of 1-runs,  $\{(l_0, l_1), (l_2, l_3), \dots, (l_{i-1}, l_i), \dots, (l_{r-1}, l_r)\}$ . Assume that this function is first displaced to  $f(x-\bar{x})$ , then sampled to obtain  $p(x)$ ,  $x \in Z$ . We wish to examine the precision by which the shift  $\bar{x}$  (the shift in the centroid) can be estimated from the sampled sequence. In a currently unpublished work, it was shown that, given  $f(x)$ , such that  $l_i - l_{i-1} > 1$ , the displacement can be determined within a maximal uncertainty interval given by,

$$E(\bar{x}) = \bar{x} \pm \frac{1}{2(r+1)}, \text{ for } l_i = n_i + \frac{i}{r+1}, n_i \in Z. \quad (9)$$

The criterion of  $l_i - l_{i-1} > 1$  guarantees that each ring is separated sufficiently that they can be differentiated. We call this, "topology preservation". Therefore in equation (9), the  $n_i$  are integer lengths that can be arbitrarily chosen after meeting this topology preservation requirement. To extend these results to the two-dimensional case, each adjacent disk should be spaced  $n_i + i / (r+1)$  apart, for inner to outer disks,  $i = 1, \dots, r$ .

One remark on the similarity of the one-dimensional approach with the concentric estimation method in this paper, is that the "topology-preservation" requirement is analogous to the approach of treating the concentric fiducial as superimposed disks. If the centroid is calculated just of all the 1-values in the concentric fiducial (that is, without considering topology) then the estimate will actually have poorer location precision (due to fewer pixels) than for the filled disk; but when topology is retained (that is, each disk is found from its associated ring) then the effective area is increased, and the precision of the centroid estimate increases as well.

### 5. Concentric Fiducial — Experimental Results

Tests were made on the performance of the concentric fiducial for subpixel translations on a sampling plane, and with noise. For these, the centroid was measured from the sampled, binary image, and the Euclidean distance between the true centroid and the measured centroid was calculated, and called the *error*. Two sets of tests were carried out. In one, a noiseless fiducial was shifted in subpixel increments on the sampling plane, and the error due to sampling determined. In the other, noise was added to the image, and the error due to this noise found.

For the determination of the effects of sampling, the center of the concentric fiducial was shifted uniformly within (0,0) to (0.5,0.5) pixels at increments of 0.01 pixels in x and y, and the maximum error was found as described in Section 2. Concentric fiducials of three outer diameters,  $d_r = \{50, 100, 300\}$ , and with a number of rings,  $r = \{1, 3, 5, \dots, 29\}$ , were tested.

The results are plotted in Figure 4. Note first that, as the number of rings is increased, the maximum error generally decreases. Also, for larger diameters, the error peaks are generally lower. However, also note that the plots are not smooth. We will discuss these apparent anomalies as well as the general trends in Section 6.

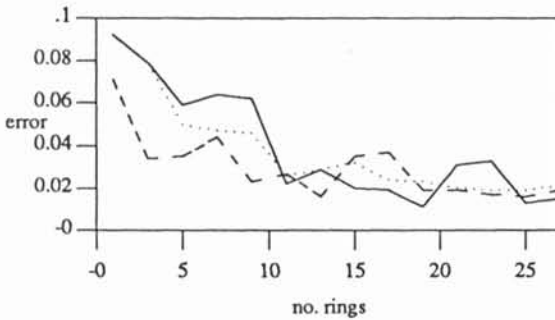


Figure 4. Maximum sampling error for concentric fiducial. Solid line is for outer ring size of 50, dashed for 100, and dotted for 300.

For the second set of tests, the fiducial was centered at (0,0), and noise introduced with the following characteristics. At each pixel location, noise was added with probability  $P$  of setting the value to 1 or 0. This yields a random spatial distribution of 1-valued noise outside the fiducial area, and 0-valued noise within the fiducial area. A range of noise probabilities was tested, but shown here is only  $P = 0.1$ . After the noise is added, a simple morphological filter was applied to reduce isolated 1 or 0 noise, and to smooth spurs and indentations on boundaries. Thus, the addition and reduction

of noise leaves rings with noisy boundaries. For each test case, 15 images were taken with different random noise. The results show the average and the standard deviation of the maximum errors over the 15 sample images of each case.

The results are plotted in Figures 5 and 6. They indicate that: i) both the error and standard deviation generally decrease when the number of rings increases; ii) error is generally smaller for larger diameters; and (from results not shown here) iii) these results are more pronounced for higher noise probability. Although the general trends are clear, the results again are not monotonic, and this will be discussed in the next section.

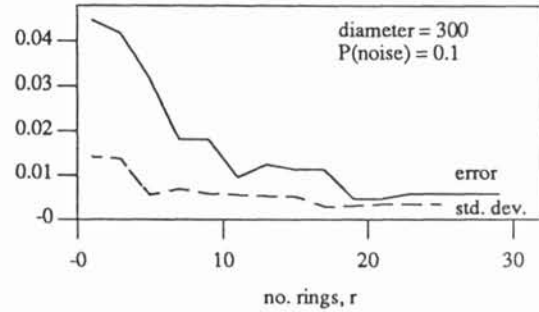


Figure 5. Plot shows average and standard deviation of maximum error versus number of rings for concentric fiducials of diameter 300, with added noise 10%.

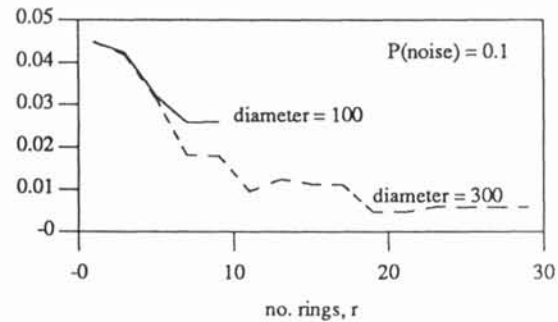


Figure 6. Plot shows average of maximum error versus number of rings for concentric fiducials of diameters 100 and 300, with added noise 10%. (Note that the plot for the diameter of 100 is only up to 9 rings. This is because pixel spacing between rings becomes too small to preserve topology.)

To test the effects of ring spacing and diameter, the error was measured for different ring widths. Error for concentric disks was calculated and plotted for diameters of:  $\{(2i-1)\Delta d + i / (1+r)\}$ , the optimum spacing for the one-dimensional case discussed in Section 4;  $\{(2i-1)\Delta d + 1/2\}$ , the optimum diameter for a single disk cross-section; and  $\{(2i-1)\Delta d\}$ , the diameter giving the worst error for a single cross-section (from the results for a square in Section 2). The maximum error due to sampling was found for the noiseless fiducial that is shifted by 0.01 pixel increments within (0,0) to (0.5,0.5).

The results are shown in Figure 7. The plots for diameters  $\{(2i-1)\Delta d + i / (1+r)\}$ , and  $\{(2i-1)\Delta d + 1/2\}$  are similar, and it would be difficult to say whether one of these diameter spacings is better than the other. For greater than one ring, however, integer diameters  $\{(2i-1)\Delta d\}$  give noticeably worse error. These results will be discussed in Section 6.

### 6. Discussion and Summary

The data indicate the following general trends for the concentric fiducial:

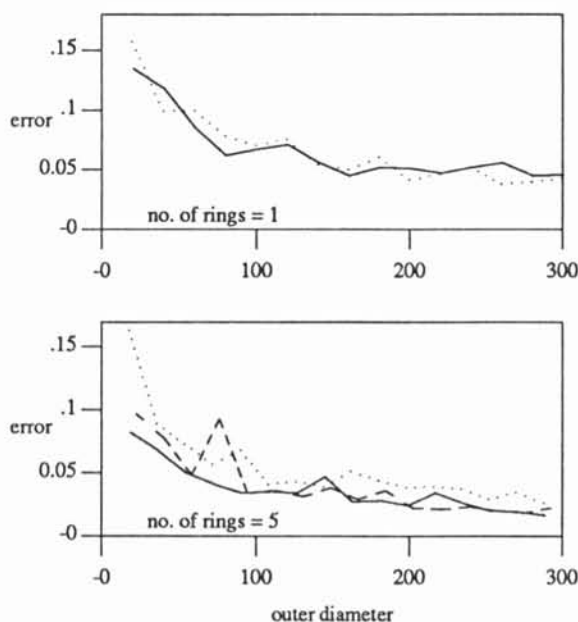


Figure 7. Maximum sampling errors for different ring spacings versus diameters for fiducial with one ring on top and five rings on bottom. Diameters are plotted:  $\{(2i-1)\Delta d+i/(1+r)\}$  (solid),  $\{(2i-1)\Delta d+1/2\}$  (dashed), and  $\{(2i-1)\Delta d\}$  (dotted).

- i. as the diameters are increased, the error due both to sampling and additive noise decreases;
- ii. as the number of rings is increased, the error due both to sampling and additive noise decreases;
- iii. as the amount of additive noise is increased, the trends of (i) and (ii) are more pronounced (this result was not shown here, see [2]);
- iv. as the number of rings is increased, the standard deviation of the error measurement due to additive noise is decreased; and
- v. ring diameters of  $\{(2i-1)\Delta d+1/(1+r_i)\}$  and  $\{(2i-1)\Delta d+1/2\}$  yield similar errors, and integer diameters worse errors.

Although the general trends are as above, in no case are they monotonic. For the plots of error due to additive noise, there are local peaks and valleys. An explanation is that some correlation exists between the sampling resolution and concentric pattern at certain number of rings and diameter sizes. This is similar to the analytical explanation for the peaks in error for the diamond shape plotted in Figure 1. However, the relationship between the circle and the sampling plane is non-linear for different shifts, diameters, and number of rings, and has so far defied analysis. A mathematical explanation for the results of Section 5 is essential to understanding and designing the optimum concentric fiducial, and it is this problem that most warrants future research.

For the plots of error due to sampling only, the general trends are observed as listed. However there are instances of more marked non-monotonicity than for the case of additive noise. We propose that this is due to the sampling effects as mentioned above.

The results in Figure 7 show that different diameters of  $\{(2i-1)\Delta d+1/(r+1)\}$  and  $\{(2i-1)\Delta d+1/2\}$  have similar errors. However, while the relative diameter spacing does not seem to be critical, it seems that when all disks have integral diameters, the maximum error is higher. This is probably due to the same effect as for the square with integral sidelengths. The effect is smaller for the circle because the sides are approximately perpendicular to a sampling axis for a smaller

portion of the sides than for a square (whose sides are exactly perpendicular for the entire sidelengths). Again, this argument requires analytical verification.

As is evident from the above discussion, efforts to describe the behavior of concentric disks in a sampling plane have so far escaped our mathematical explanation. The difficulty of the problem is also evident from the literature. This problem is broached in [7], but due to the difficulty of analysis, no general two-dimensional relationship was obtained. In [4], a discrete disk is analyzed, but this is done only for the more restricted case where the center is fixed on a sample point. In [3,8], it is evident that their locale, describing the region of imprecision, becomes more complex with increased region samples. The problem appears to be non-linear because the circular edges of the disks are uncorrelated with the Cartesian sampling plane. In any case this problem merits future effort.

In summary, it has been shown that the circular fiducial used for machine vision registration can be extended to a concentric pattern that occupies the same area, but yields better centroid estimates. A method of centroid calculation was shown that treats the fiducial with  $r$  concentric rings, as  $r$  separate but concentric disks, thus yielding a larger effective area and a lower effective variance. Experiments were performed to find the error in the centroid measurement due to additive noise, and due to sampling quantization. These showed that the centroid measurement was generally more accurate as the outside diameter and number of concentric rings increased. Although the benefits of this shape and method for registration have been shown by experiment, a challenging problem still remains to explain by analysis some non-monotonicities in the results.

#### REFERENCES

1. C.B. Bose, I. Amir, "Design of fiducials to facilitate inspection using machine vision", IEEE Trans. PAMI, Nov., 1990.
2. L. O'Gorman, A.M. Bruckstein, C.B. Bose, I. Amir, "Subpixel registration using a concentric ring fiducial", Int. Conf. Pattern Recognition, June, 1990, Atlantic City, USA, pp. 249-332.
3. D.I. Havelock, "Geometric precision in noise-free digital images", IEEE Trans. PAMI, PAMI-11, No. 10, Oct. 1989, pp. 1065-1075.
4. Z. Kulpa, "On the properties of discrete circles, rings, and disks", Computer Vision, Graphics, and Image Processing, Vol. 10, 1979, pp. 348-365.
5. A. Nakamura, K. Aizawa, "Digital Circles", Computer Vision, Graphics, and Image Processing, Vol. 26, 1984, pp. 242-255.
6. D.I. Havelock, "The topology of locales and its effects on registration noise", submitted to IEEE Trans. PAMI, 1990.
7. J.W. Hill, "Dimensional measurements from quantized images", in *Machine Intelligence Research Applied to Industrial Automation*, by D. Nitzan, et al., SRI 10th Report for NSF Grant DAR78-27128, 1980, pp. 75-105.
8. L. Dorst, A.W.M. Smeulders, "Discrete representation of straight lines", IEEE Trans. PAMI, PAMI-6, No. 4, July, 1984, pp. 450-462.